BL2B

Performance Test of Z-Stack MCP Mounted in a TOF Mass Spectrometer

C. Huang[1], H. Katayanagi[1,2], Md. S. I. Prodhan[2], H. Yagi[1], B. P. Kafle[2], K. Mitsuke[1,2]
[1]*Institute for Molecular Science, Myodaiji, Okazaki 444-8585, Japan*
[2]*Graduate University for Advanced Studies, Myodaiji, Okazaki 444-8585, Japan*

The microchannel plates detector (MCP) is a kind of universal and traditional tool which is used for detection of photons and charged particles in a large variety of applications including imaging spectroscopy, electron spectroscopy, mass spectrometry, astronomy, molecular atomic collision studies, cluster physics and so on. The detection efficiency (η) of MCP is a very important parameter and is known to be a complicated function of the kinetic and internal energies and the mass to charge ratio (m/z) of impinging particles and the bias voltage. As for the conventional two-stage MCP, the η value decreases rapidly with the increase of m/z at m/z >150.[1] Compared with the two-stage MCP, the η of z-stack MCP (three-stage MCP) is much easier to be saturated.

Recently we have replaced the two-stage MCP in our TOF mass spectrometer by a three-stage MCP which includes three microchannel plates at the BL2B endstation of UVSOR. Some rare gases, i.e. helium, neon and krypton are utilized to test the performance of the new MCP. In the experiment, the output signal from the MCP was amplified with a preamplifier (EG&G, Ortec, 9301, gain=10) and an amplifier (EG&G, Ortec, 9302, gain=20), then discriminated by a constant fraction discriminator (EG&G, Ortec, 474). After the discrimination, the signal was processed by a time-to digital converter (FastComtec, 8867). Ion counts were normalized by photonflux and sample pressure to evaluate the relative η value.

Here we show the results of Kr as an example. In the experiment, the normalized signal counts of singly, doubly and triply charged ions of Kr were attained using several MCP bias voltage at $h\nu$=90eV. Fig 1 shows the dependence of normalized signal counts of Kr on the discriminator level when the MCP bias voltage is set to -2.7kV, -2.8kV, -2.9kV and -3.0kV.

In this figure, the normalized signal counts of individual Kr^{z+}(z=1-3) ions are almost the same when the discriminator level increases from 200 mV to 600 mV and the MCP bias voltage changed from -2.7kV to -3.0kV. At a given discriminator level, the count rate of Kr^{z+}(z=1-3) ion signal do not depend on the bias voltage. The same results were found in the helium and neon results. The ratios between multiply charged ions and singly charged ions of these rare gases were kept almost constant with the change of the discriminator level and bias voltage. Therefore, we concluded that η of z-stack MCP is made to operate in a saturate manner in the broad range of discriminator level and MCP bias voltage. Finally we determined the relative ion counts of C_{60}^{z+} (z=1-3) and their concomitant fragment ions. The η is saturated when the bias voltage is set to above 2.95 kV.

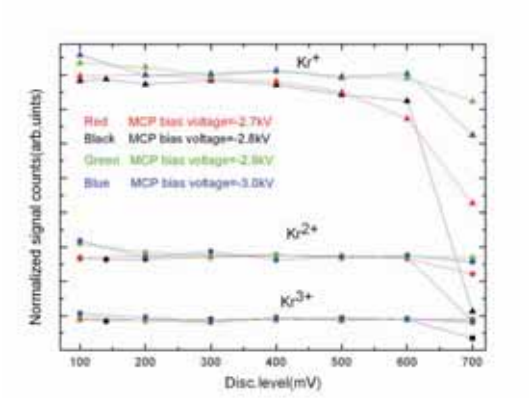

Fig. 1. The dependence of normalized signal counts on the discriminator level at different MCP bias voltages.

[1] K. Mitsuke *et al* J. Phys. Chem. A **111** (2007) 8336.

BL2B

Development of a New Momentum Imaging Spectrometer with the Use of Synchrotron Radiation Photoionization

C. Huang[1], H. Katayanagi[1,2], Md. S. I. Prodhan[2], H. Yagi[1], B. P. Kafle[2], K. Mitsuke[1,2]

[1]*Institute for Molecular Science, Myodaiji, Okazaki 444-8585, Japan*

[2]*Graduate University for Advanced Studies, Myodaiji, Okazaki 444-8585, Japan*

A novel momentum imaging spectrometer has been constructed to investigate dissociation mechanism of fullerenes molecules combining synchrotron radiation photoionization in the VUV in BL2B of UVSOR. The structure of the new apparatus is similar to the conventional velocity map imaging spectrometer developed by Eppink and Parker [1].

The performance of the spectrometer has been tested by using the He, Ne, Ar, Kr, SF_6 and CF_4. The best focusing condition was found to be

$$\frac{V_{ext} - V_{tub}}{V_{rep} - V_{tub}} = 0.7 .$$

Here V_{ext}, V_{rep} and V_{tub} correspond to voltages which applied to TOF extractor plate, TOF repeller plate and TOF tube respectively.

Figure 1 is the image of the Kr ions which was measured at the best focusing condition at $h\nu$=35eV. The inverse abel transform (IAT) [2] was applied to analyze all the image data. In the data processing, Welch window was used to suppress background noise. The velocity distribution of the projected ions was extracted from the raw data by using IAT method.

The Maxwell-Boltzman distribution of all of the rare gas ions has been calculated at the room temperature (300K). Comparing the velocity distribution of rare gas ions with the calculated Maxwell-Boltzman distribution, we found our experimental results agree with the calculated distribution Fig.2 shows the velocity distribution of Xe^{z+}(z=1-3).

Very recently, the first imaging data of the C_{60} ions have been achieved using the imaging setup in BL2B [3].

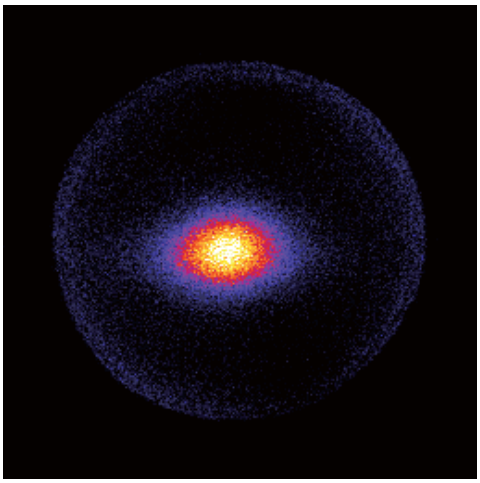

Fig. 1. The imaging of Kr ions which were measured at the best focusing condition at $h\nu$=35eV.

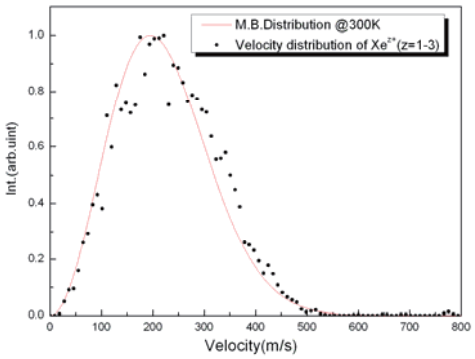

Fig. 2. The velocity distribution and the Maxwell-Boltzman distribution at 300K of Xe^{z+}(z=1-3).

[1] A. T. J. B. Eppink, D.H. Paker, Rev. Sci. Instrum. **69** (1997) 3477.

[2] A. J. R. Heck, D. W. Chandler, Annu. Rev. Phys. Chem., **46** (1995) 335.

[3] H. Katayagagi, *et al*, in preparation.

BL2B

Evaluation of the Optical Oscillator Strength of C_{60} in the Valence Region

B. P. Kafle[1], H. Katayanagi [1,2], S. I. Prodhan[1], H. Yagi [2], C. Huang [2], K. Mitsuke [1,2]

[1]*Graduate University for Advanced Studies, Okazaki 444-8585, Japan*

[2]*Department of Photo-Molecular Science, Institute for Molecular Science, Okazaki 444-8585, Japan*

We have reevaluated the absolute partial cross section $\sigma_{abs}(z+)$ for the formation of the ions in a charge state z from C_{60} [1], by applying essentially the same method as that employed in our previous studies for estimating $\sigma_{abs}(z+)$ (z = 1 - 3) at $h\nu$ = 25 to 120 eV ([2] and refs. therein). Specifically, the absolute partial cross section $\sigma(z+)$ for the formation of C_{60}^{z+} can be expressed as

$$\sigma_{\mathrm{abs}}(z+) = \frac{R(z+)}{\Phi n L F \tau} \cdot \frac{1}{\eta_{\mathrm{abs}}(z+)} . \quad (1)$$

Here, $R(z+)$ is the signal count rate of the photoions in a charge state z produced from C_{60}, Φ is the photon flux of synchrotron radiation, n is the number density of C_{60} in the ionization region, L is the length of the ionization volume along the light path, F is the repetition rate of the pulsed electric field, τ is the average residence time of the ions in the ionization volume under the field free condition. Open circles, triangles, and squares in Fig. 1 indicate, respectively, the absolute partial cross sections σ(+), σ(2+), and σ(3+) for the formation of C_{60}^{+}, C_{60}^{2+}, and C_{60}^{3+} from C_{60}. Each partial cross section includes the contribution of not only the parent but also fragment ions produced by the sequential loss of a C_2 unit. Hence, it is equal to the cross section involving all the ionic species in a particular charge state.

In Fig. 2, open circles represent the sum of $\sigma_{abs}(+)$, $\sigma_{abs}(2+)$, and $\sigma_{abs}(3+)$ which is nearly equal to the total photoionization cross section $\sigma_{abs,I}$. In the $h\nu$ range from ~ 45 to 120 eV the present curve of $\sigma_{abs,I}$ is in fair agreement with the $\sigma_{abs,I}$ reported by Reinköster *et al.* [3] and absolute photoabsorption cross section curve $\sigma_{abs,A}$ by Colavita *et al.* [4]. This may prove the validity of our data analysis. Our $\sigma_{abs,I}$ of 401 Mb at $h\nu$ = 25.5 eV is a little smaller than $\sigma_{abs,A}$ determined by Jaensch and Kamke [5].

The oscillator strength f was calculated, by combining the present $\sigma_{abs,I}$ curve with the $\sigma_{abs,A}$ data given in Ref. [5] ($h\nu$ = 11.4–25 eV) and Yasumatsu *et al.* ($h\nu$ = 3.5–11.4 eV) [6]. The value integrated over the $h\nu$ range from 3.5 to 40.8 eV was 120.4 and that from 3.5 to 119 eV was 156.0. These values are significantly smaller than the corresponding oscillator strengths of 187.6 and 233.4 expected from the TKR sum rule and 60 times the total photoabsorption cross section of a C atom, 60×σ(C) [7]. The insufficiency of f is entirely predictable because the $\sigma_{abs,A}$ data points of Ref. [5] lie much lower than those compiled by Berkowitz [7]. Many authors have argued that the most dependable equilibrium vapor pressures of C_{60} were given by Piacente *et al.* in 1995 [8]. By using their vapor pressure data, we have reevaluated $\sigma_{abs,A}$ of Refs. [5] and [6]. As a result the f values were recomputed to be 178.5 and 230.5 for the $h\nu$ ranges, respectively, from 3.5 to 40.8 eV and from 3.5 to 119 eV. These values agree well with those expected from the TKR sum rule and 60×σ(C), namely 187.6 for the former range and 233.4 for the latter range.

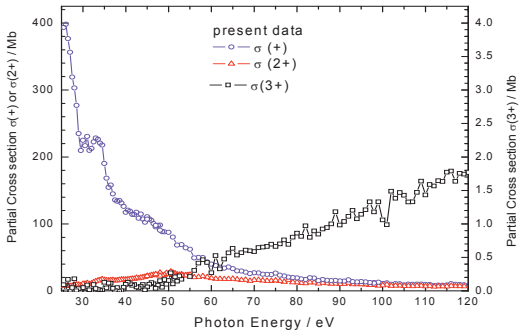

Fig. 1. Partial cross sections for single, double and triple photoionization of C_{60} determined from eq. (1).

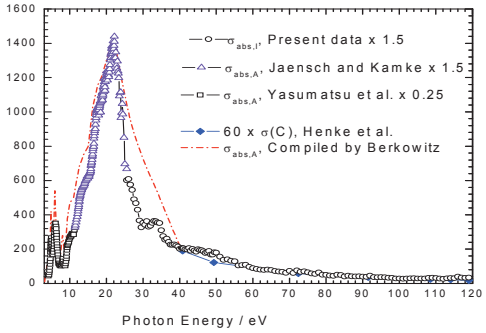

Fig. 2. Total photoionization and photoabsorption cross sections of C_{60} in the $h\nu$ range of 3.5–119 eV.

[1] B. P. Kafle *et al.*, J. Phys. Soc. Jpn. **77** (2008) 014302.
[2] K. Mitsuke *et al.*, J. Phys. Chem. A **111** (2007) 8336.
[3] A. Reinköster *et al.*, J. Phys. B **37** (2004) 2135.
[4] P. Colavita *et al.*, Phys. Chem. Chem. Phys. **3** (2001) 4481.
[5] R. Jaensch, W. Kamke, Mol. Mater. **13** (2000) 143.
[6] H. Yasumatsu *et al.*, J. Chem. Phys. **104** (1996) 899.
[7] J. Berkowitz, J. Chem. Phys. **111** (1999) 1446.
[8] V. Piacente *et al.*, J. Phys. Chem. **99** (1995) 14052.

BL2B

Velocity Map Imaging of C_{60} Molecular Beams

H. Katayanagi[1,2], C. Huang[1], S. I. Prodhan[2], H. Yagi[1], B. P. Kafle[2], K. Nakajima[3], K. Mitsuke[1,2]

[1]*Department of Photo-Molecular Science, Institute for Molecular Science, Okazaki 444-8585, Japan*

[2]*Graduate University for Advanced Studies, Okazaki 444-8585, Japan*

[3]*Faculty of Letters, Hosei University, Chiyoda-ku, Tokyo 102-8160, Japan*

The photoion images of fullerene (C_{60}) molecular beams were observed with the velocity map imaging technique [1]. The temperature of the beam was derived from the images and was consistent with that of the fullerene oven.

The design of our imaging setup was described elsewhere [2]; here we explain the experimental procedure briefly. The C_{60} sample was loaded in a cylindrical quartz cell and heated up by a heater around 700-800 K in vacuum. The C_{60} vapor passed through two apertures and reached the ionization region, where the C_{60} molecular beam intersected the monochromatized synchrotron radiation. Ions produced at the ionization region were extracted by a velocity map imaging electrode assembly and projected on to a position sensitive detector (PSD) of 25 mm in diameter and 375 mm away from the ionization region. No mass selection was made. We thus obtained two-dimensional (2D) projections of three-dimensional (3D) scattering distributions of the ions on the PSD. Focusing conditions of this electrode assembly were determined in advance using rare gases at room temperature as samples.

An image of the ions produced by photoionization of C_{60} at the photon energy of 70 eV is shown in Fig. 1a. The synchrotron radiation passes parallel to the abscissa and the C_{60} beam to the ordinate of the image. The image is parallel to the plane spanned by the synchrotron radiation and the C_{60} beam. Spatial distributions of C_{60}^+ directly reflect those of parent C_{60} in the beam. An acute vertical intense part is clearly observed at the center of the image. This part can be assigned to a projected shape of the C_{60} beam, or a 2D projection of 3D velocity and angular distribution of the beam, because the intensity of this part changed with changing the sublimation rate of C_{60} which can be controlled with the adjustment of the oven temperature. Around the "base" of the acute component, a subtle round component also exists. We considered that this component originated from ionized residual gases and, if any, fullerene vapor which stagnates around the ionization region. The acute component shows cylindrical symmetry around its major axis since the fullerene beam source mechanically has cylindrical symmetry.

We tried to derive the velocity distribution, or the temperature of the C_{60} beam from the present results. We measured a background image experimentally without fullerene evaporation and subtracted it from the image with fullerene evaporation. We regarded the major axis of the acute component as a cylindrically symmetric axis and applied the inverse Abel transform with which we can calculate a 2D section of the 3D distribution [3]. On the section, distance from an origin of the image is directly proportional to velocity. The origin and a coefficient to convert the distance into velocity were obtained from the ion images of Kr at room temperature. The velocity distribution of C_{60} beam is shown in Fig. 1b. Solid curve in Fig. 1b shows shifted Maxwell-Boltzmann (MB) distribution of which temperature was set to the same as that of the fullerene oven. The experimental distribution agreed well with the MB distribution with a small shift of 15 m/s.

As a result of the present experiment, we concluded that our imaging setup worked well even with fullerenes. We will observe photofragment ion images from fullerenes in order to investigate the dynamics of dissociative photoionization of fullerenes. In addition, an establishment of the present beam diagnostic method of evaporating fullerenes will allow us to design a new type of beam monitor for MBE or CVD experiments.

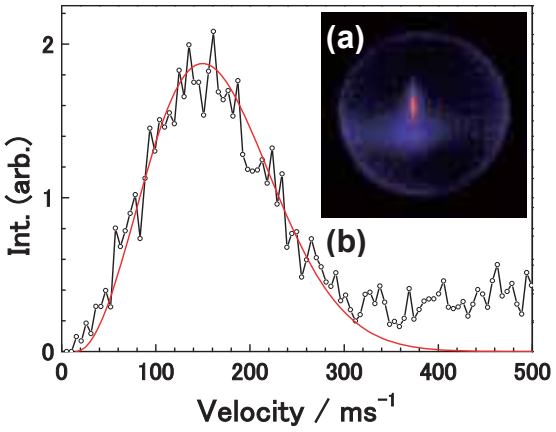

Fig. 1. (a) Ion image of C_{60} beam. (b) Velocity distribution of C_{60} beam. Black curve shows velocity distribution of C_{60} beam derived from (a), red curve shows MB distribution of 785 K with a shift of 15 m/s.

[1] A. T. J. B. Eppink, D. H. Parker, Rev Sci. Instrum. **68** (1997) 3477.

[2] B. P. Kafle *et al.* AIP Conf. Proc. **879** (2007) 1809.

[3] S. M. Candel et al. Comput. Phys. Commun. **23** (1981) 343.

BL2B

Total Electron Yield Spectroscopy and Electron-Signal-Triggered TOF Mass Spectrometry Developed for the Studies on Photodissociation Dynamics of Fullerens

H. Katayanagi[1,2], C. Huang[1], S. I. Prodhan[2], H. Yagi[1], B. P. Kafle[2], K. Nakajima[3], K. Mitsuke[1,2]

[1]*Department of Photo-Molecular Science, Institute for Molecular Science, Okazaki 444-8585, Japan*

[2]*Graduate University for Advanced Studies, Okazaki 444-8585, Japan*

[3]*Faculty of Letters, Hosei University, Chiyoda-ku, Tokyo 102-8160, Japan*

In order to detect all the photoelectrons from fullerenes, we modified a threshold electron analyzer [1] which could be attached easily at the opposite side of ion time-of-flight (TOF) and imaging spectrometers [2]. The performance of the modified electrodes as a total electron detector was inspected by measuring total electron yield (TEY) spectra and electron-signal-triggered ion TOF mass spectra of Kr.

We originally designed and produced the threshold electron analyzer to perform threshold electron photoion coincidence (TEPICO) experiments in order to clarify the dynamics of dissociative photoionization of fullerenes (C_{60}, C_{70}, etc.) [1]. The TEPICO experiments will allow us to determine the internal energies of parent ions uniquely. Meanwhile, we utilize the total electron detector for the following purposes: (1) supplying start triggers in the imaging experiments to select masses of ions imaged, (2) measuring the absolute photoionization cross sections of fullerenes from their TEY spectra. This method is more advantageous from the total ion yield (TIY) measurements, because the detection efficiency of a microchannel plate detector depends on the mass-to-charge ratios (m/z) of fullerene ions.

We have revised the former electron analyzer so as to make it applicable to the total electron detector by enlarging the diameters of the holes on lenses and applying higher voltage to the lenses and even to a stray electron shield covering the electrodes.

We measured TEY spectra of Kr in the photon energy range of 90-96 eV. The Kr sample was introduced to the chamber through a needle valve. A typical pressure in the chamber was 2×10^{-6} Torr. Figure 1 shows a typical TEY spectrum of Kr. This spectrum agrees very well with the TIY spectra measured at BL2B previously [3], except a small rise of the baseline because of stray electrons.

We also tried to measure TOF spectra of Kr^{z+} ions using the electron signal as a start trigger. Figure 2 shows a thus obtained TOF spectrum of Kr^{z+} at the photon energy of 55 eV. Peaks of singly and doubly charged Kr ions are clearly observed. The peaks have tails toward the longer flight time, which indicates a finer voltage adjustment is required. The peak area ratio of $(Kr^{2+})/(Kr^{+})$ is much larger than that we expected according to Ref. 4. This can be explained as a composite effect of the following reasons: doubly charged ions emit two electrons and thus double the probability of triggering, and the present electron detector has higher efficiency for the slower electrons produced by double ionization. The earlier peaks at flight times of 5.0 and 6.2 μs are probably due to residual water and nitrogen in the chamber. Although N_2 has almost the same m/z ratio as that of Kr^{3+}, the peak at 6.2 μs can be assigned to N_2^+ since the threshold for the triple ionization of Kr is 75 eV.

In summary, we concluded that this electron detector can be used to observe electrons from fullerenes of which number density is at most one order of magnitude smaller than those of rare gases, although further tuning of the detector will be needed.

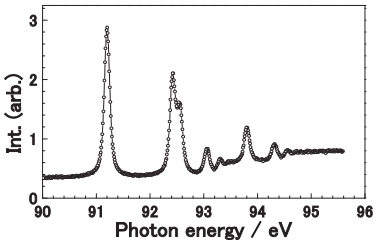

Fig. 1. Total electron yield spectra of Kr in the photon energy range of 90-95.6 eV. Peaks can be assigned to the $3d^{-1}{}_{5/2}$ and $3d^{-1}{}_{3/2}$ series.

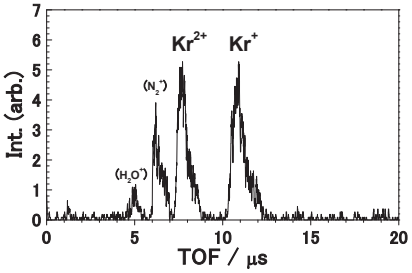

Fig. 2. Electron-signal-triggered TOF spectra of Kr^{z+} at the photon energy of 55 eV.

[1] H. Katayanagi *et al*., UVSOR Activity Report **33** (2006) 46.

[2] B. P. Kafle *et al*., AIP Conf. Proc. **879** (2007) 1809.

[3] M. Ono *et al*., Nucl. Instrum. Methods Phys. Res. A **467-468** (2001) 577.

[4] N. Saito, H. Suzuki, Int. J. Mass Spectrom. Ion Proc. **115** (1992) 157.

BL2B

Momentum Imaging of the Photofragments from C_{60} and Data Analysis of the Image

S. I. Prodhan[1], H. Katayanagi[1,2], B. P. Kafle[1], C. Huang[2], H. Yagi[2], K. Mitsuke[1,2]
[1]*The Graduate University for Advanced Studies Okazaki 444-8585, Japan*
[2]*The Institute for Molecular Science, Okazaki 444-8585, Japan*

We have developed a time-of-flight (TOF) based mass-selected momentum imaging spectrometer to observe the momentum distributions of the scattered fragments produced from dissociative photoionization of gaseous C_{60} at the BL2B in the UVSOR facility. We have adopted the Eppink-Parker type three-element velocity focusing lens system [1] (Repeller, Extractor, and Tube electrodes) to achieve the high kinetic energy (KE) resolution on the photofragment images. It is known that two possible mechanisms are proposed for the fragmentation processes [2,3], namely the sequential ejection of C_2 units as $C_{60}^+ \rightarrow C_{58}^+ + C_2$, $C_{58}^+ \rightarrow C_{56}^+ + C_2$, and the fission of C_{60}^+ to directly produce a final fragment as $C_{60}^+ \rightarrow C_{56}^+ + C_4$.

Several groups tried to distinguish the above two mechanisms by measuring the total average KE release in the decomposition of C_{60} into its fragments [4,5], though such efforts have met with failure because the two mechanisms give almost the same total average KE release. It is likely that expanding C_{56}^+ ion clouds arising from different reaction mechanisms give different shapes of image or different momentum distributions of C_{56}^+. We examined this statement by means of computer simulation and designed the momentum imaging apparatus [3] which is now installed in our experimental end station of BL2B.

In the momentum imaging technique the 3D momentum distributions of fullerene photofragment ions are projected on the 2D position sensitive detector (PSD). We performed the Monte Carlo simulation to generate the momentum images under the following conditions: TOF, 50μs; number of ions hitting at the surface of PSD, 8×10^5; temperature of the C_{60} molecular beam, 0K and 273K. The KE release in the C_2 or C_4 ejection takes a constant value of 0.4 eV, to a first approximation. Angular distribution is assumed to be isotropic and angles of ejection are selected randomly.

The simulated images of the fragment ion C_{56}^+ from C_{60} through the C_2 loss and C_4 loss mechanisms are depicted in Fig. 1. Obviously the two mechanisms are well distinguished at 0 K, but with increasing temperature they are hardly distinguishable. The experimental image of C_{56}^+ is a convolution of the momentum distribution of the parent C_{60} in the beam and that of C_{56}^+ produced by the reaction. We can observe the image of the parent C_{60}^+ (momentum distribution of C_{60} in the beam), as well as that of C_{56}^+. Thus, we are trying to deconvolute the effect of the initial C_{60} beam temperature by analyzing the image data.

We are carrying out experiments with C_{60} sample for checking the performance of the newly installed imaging spectrometer. The C_{60} and background images recently measured are shown in Fig. 2. The experimental conditions are given in the caption.

Fig. 1. Simulated 2D projections of the 3D scattering

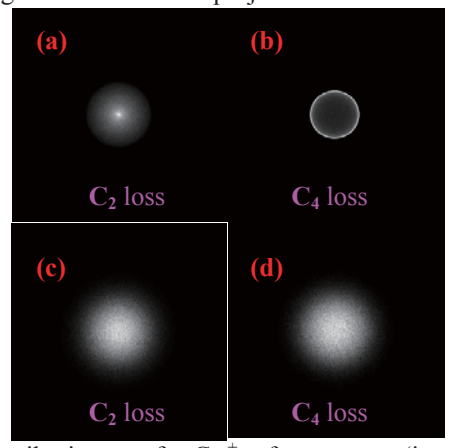

distributions of C_{56}^+ fragments (image size: 40×40mm). (a) and (c), sequential ejection of C_2 units; (b) and (d), fission of C_{60}^+. The beam temperature is 0K for (a) and (b) and 273K for (c) and (d).

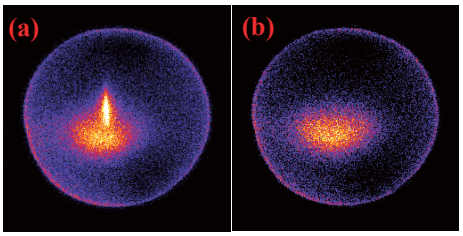

Fig. 2. (a) The experimental C_{60} image at beam temperature, 505.2°C (b) Background image at room temperature, 27°C. Photon energy,90eV; V_{MCP}, -2.2KV; V_{tube}, -350V; V_{rep}, 500V; V_{ext}, 250V; V_{deft}, 25V; data acquisition time, 60s.

[1] A.T. J. B. Eppink, D. H. Parker, Rev. Sci. Instrum. **68** (1997) 3477.
[2] K. Mitsuke *et al.*, AIP Conf. Proc. **811** (2006) 161.
[3] B. P. Kafle *et al.*, AIP Conf. Proc. **879** (2007) 1809.
[4] H. Gaber *et al.*, Z. Phys. D **24** (1992) 302.
[5] D. Muigg *et al.*, J. Chem.Phys. **108** (1998) 963.

BL3U

X-Ray Absorption Spectra of Small Kr Clusters: Mass-Selected Ion Yields with a TOF Spectrometer

M. Nagasaka, T. Horigome, T. Hatsui, N. Kosugi
Institute for Molecular Science, Myodaiji, Okazaki 444-8585, Japan

The cluster is an intermediate phase between isolated and condensed ones and has both properties of surface and bulk dependent on its size. Inner-shell spectroscopies such as X-ray absorption and photoelectron (XAS, XPS) are promising methods to investigate local, or site-selected, electronic structures [1, 2]. XAS and XPS of large clusters (average size N > 1000) show dominant bulk and surface features of clusters [1]. On the other hand, XPS of small clusters (N < 100) efficiently reveals several kinds of surface sites [2]. The site dependence in XAS of small clusters may be possible in neither total electron nor ion yield, because the amount of clusters is relatively low compared to monomers and dimers involved inherently in the adiabatic gas expansion. A component of small clusters should be extracted from the cluster/monomer/dimer mixture. In the present work, we have developed a compact time-of-flight (TOF) mass spectrometer to measure Kr_2^+ yields emitted from small clusters and then to obtain mass-selected ion yield spectra, which correspond to selective or enhanced XAS for small Kr clusters.

Kr clusters were produced by the adiabatic gas expansion. The gas was expanded through a 50 μm nozzle into vacuum with the stagnation pressure of 0.5 MPa, where the average size of Kr clusters was about 30. The Kr clusters were ionized or excited near the Kr $3d_{5/2}$ and $3d_{3/2}$ edges by using monochromatic soft x-rays from the high-resolution undulator beamline BL3U. In the present work, to get higher photon fluxes, photon energy band path was set to ~40 meV. To get XAS of small Kr clusters, the Kr_2^+ ions emitted from clusters after photoabsorption were collected as a function of photon energy by using a newly developed Wiley-McLaren type TOF mass spectrometer [3]. Figure 1 shows a schematic TOF mass spectrometer, where Kr_2^+ was triggered by pulsed voltage apparatus with the repetition ratio of 10 kHz, secondly accelerated, traveled in the drift tube, and collected by the MCP detector. The Kr_2^+ ions were extracted from the total signals by using delay-pulse generator and constant-fraction discriminator.

Figure 2 shows XAS of Kr clusters obtained in the present method. The spectra show contributions from both Kr atoms and Kr clusters. The peaks for Kr atoms also include contributions from Kr dimers, because the electronic state of dimers is close to that of atoms [2]. In the region of the lowest excitation $3d_{5/2}^{-1}5p$, the surface peak in the small clusters is clearly observed with 0.17 eV blueshift from the

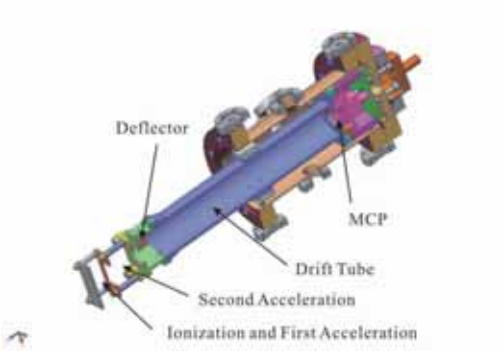

Fig. 1. Schematics of TOF mass spectrometer.

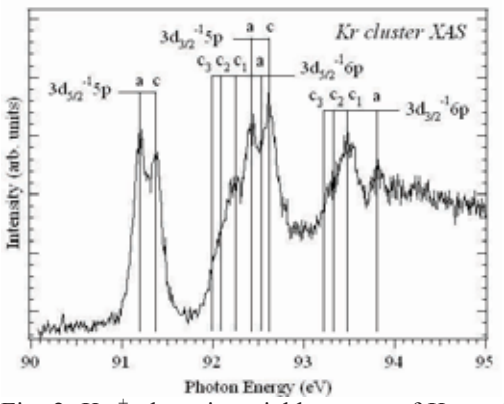

Fig. 2. Kr_2^+ photo-ion yield spectra of $Kr_{\sim 30}$ clusters, where a and c mean the Kr atoms/dimers and Kr clusters, respectively.

atomic/dimer peak. No bulk peak is observed. This blueshift is larger than the blueshift (0.13 eV) in large clusters (N ~ 4700) [1]. The cluster peaks in the $3d_{3/2}^{-1}5p$ region are also blue-shifted by 0.19 eV. On the other hand, the cluster peaks in the $3d_{5/2}^{-1}6p$ and $3d_{3/2}^{-1}6p$ regions are red-shifted by 0.29 eV and 0.32 eV, respectively, whereas 0.45 eV redshifts are reported in the $3d^{-1}6p$ peaks of large clusters [1].

The $3d^{-1}5p$ cluster peak (blue-shifted) widths are similar to the atomic/dimer ones, but the $3d^{-1}6p$ cluster peaks are broad with shoulder features c_1, c_2, and c_3 at the lower-energy part (red-shifted). In order to elucidate origin of these blue and red shifts, we are analyzing the present results by combining XPS, resonant XPS, and theoretical simulations.

[1] For example, M. Tchaplyguine *et al.*, J. Chem. Phys. **127** (2007) 124314.
[2] T. Hatsui *et al.*, J. Chem. Phys. **123** (2005) 154304.
[3] W. C. Wiley, I. H. McLaren, Rev. Sci. Instrum. **26** (1955) 1150.

BL3U

Resonant Auger Electron Spectra of Small Kr Clusters near the Kr 3d Thresholds

M. Nagasaka, T. Hatsui, N. Kosugi
Institute for Molecular Science, Myodaiji, Okazaki 444-8585, Japan

We have measured x-ray absorption spectra (XAS) of small krypton clusters (average size N ~ 30) by Kr_2^+ ion yields and successfully observed site-dependent surface $3d^{-1}np$ peaks [1]. In the present work, we applied resonant Auger electron spectroscopy (RAES) to the same small Kr clusters on the photoexcitation energies of $3d^{-1}5p$ and $3d^{-1}6p$ with distinct atom-surface energy shifts.

Kr clusters were produced by the adiabatic gas expansion through a 50 μm nozzle into vacuum with the stagnation pressure of 0.5 MPa, where the average size is estimated to be ~30, indicating only two or three bulk atoms and mostly surface atoms [1,2]. Kr clusters were excited by monochromatic soft x-rays from the undulator beamline BL3U. The photon energy band path was set to be 40 meV. RAES spectra were measured by using an electron energy analyzer, SES-200 combined with A-1 lens and detection system, with the pass energy of 100 eV [2].

Figures 1(a) and 1(b) show RAES spectra of small Kr clusters (with almost no bulk sites) by choosing the photoexcitation energies of cluster surface $3d_{5/2}^{-1}5p$ and $3d_{5/2}^{-1}6p$ transitions. In the clusters, difference between the $3d_{5/2}^{-1}5p$ and $3d_{5/2}^{-1}6p$ RAES spectra is relatively small. This may be mainly because the atomic 5p and 6p orbitals are strongly distorted and mixed in clusters. We could not remove atomic contributions in the cluster spectra.

The atomic RAES peaks are assigned according to the work of Jauhiainen *et al* [3]. We observed dominant *np* Rydberg series converging to ^{3}P, ^{1}D and ^{1}S $(4p)^4$ states, where the branching ratio is 16:53:31. This situation is also applicable to the cluster spectra; as compared with the atomic peaks, the $4p^45p$ cluster peaks are red-shifted by 0.6 eV and the $4p^46p$ cluster peaks are red-shifted by 2.1 eV. The stabilization energy in singly 3d ionized states is 0.5 eV in the same small clusters [1] and is 0.8 eV in the large clusters N = 4700 [4]. Thus, the stabilization energy of doubly 4p ionized states in the small cluster is 2.6 eV (2.1+0.5) and is 0.6 eV smaller than the corresponding atom-surface energy difference 3.2 eV in the large Kr clusters [4].

Similarly to the Kr 3d excitation spectra [1], Fig. 1 shows that the higher *np* Rydberg states (n > 6) are almost quenched in the $(4p)^4$ manifold in the cluster. Then, there may be n>>0 band-like features ("conduction band" [4]) around the single/double ionization thresholds. Normal Auger electrons from the single core hole state to doubly ionized states cannot be observed below the ionization threshold; however, resonant Auger spectra near the threshold sometimes show normal Auger-like features [4,5]. Although a 40.9 eV feature in Fig. 1(b) has not yet been successfully assigned, the peaks of 37.8 eV and 40.0 eV observed in Fig. 1(a) may be assigned to $(4p)^4np$ ^{1}D and ^{1}S with n >> 0 around the double ionization threshold. They are comparable to 37.0 and 39.3 eV double 4p ionization energies in the large cluster surface [4]. These discrepancies correspond to the difference in the stabilization energy of doubly 4p ionized states 0.6 eV as above discussed.

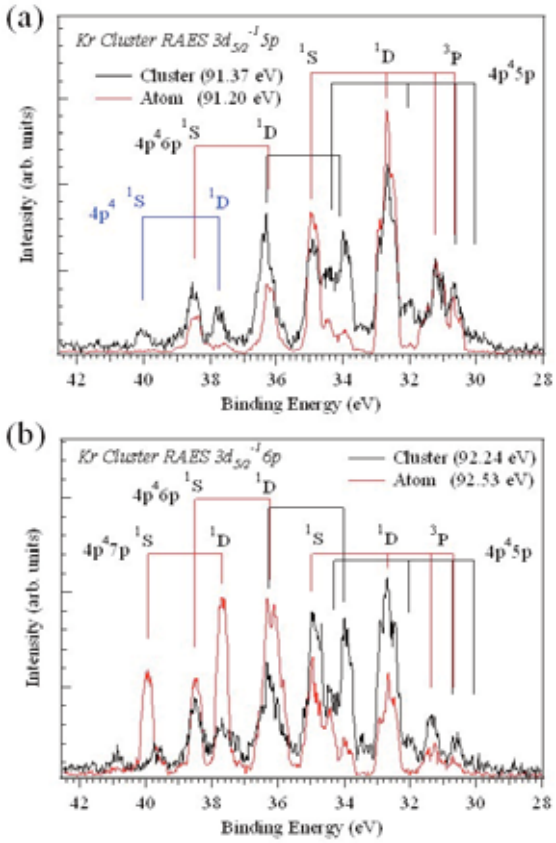

Fig. 1. RAES of Kr clusters (black line) following the (a) $3d_{5/2}^{-1}5p$ and (b) $3d_{5/2}^{-1}6p$ excitations in clusters [1], together with the atomic spectra (red line).

[1] M. Nagasaka *et al.*, in this volume.
[2] T. Hatsui *et al.*, J. Chem. Phys. **123** (2005) 154304.
[3] J. Jauhiainen *et al.*, J. Phys. B **29** (1996) 3385.
[4] M. Tchaplyguine *et al.*, J. Chem. Phys. **127** (2007) 124314.
[5] A. Kivimäki *et al.*, Phys. Rev. A **71** (2005) 033204.

BL4B

Formation of Metastable Carbonyl Sulfide (OCS) Dications Following Core-Hole Creation

M. Ito[1,2], K. Soejima[2], T. Kaneyasu[1], Y. Hikosaka[1], E. Shigemasa[1]
[1]*UVSOR Facility, Institute for Molecular Science, Okazaki 444-8585 Japan*
[2]*Graduate School of Science and Technology, Niigata University, Niigata 950-21 Japan*

While doubly charged molecular ions (or dications) are inherently unstable owing to the Coulomb repulsion between the nuclei, metastable molecular dications having lifetimes of at least μs order are known to exist from mass spectroscopic studies. In an inner-shell study of Carbonyl Sulfide (OCS), it has been reported that Auger decays of the S 2*p* core-hole states favorably populate metastable OCS^{2+}, in contrast to the case of the C 1*s* core-hole states [1]. In this study, we have used an Auger-electron-ion coincidence method to investigate formation mechanism of the metastable dications following the core-hole creations in OCS molecules.

The experiment was performed at BL4B, using the electron-ion coincidence spectrometer [2]. The electrons were analyzed in energy by a double toroidal electron analyzer, while ions were extracted from the interaction region into an ion momentum spectrometer by a pulsed electric field according to the detection of the electron. As an example, the time-of-flight (TOF) spectrum obtained in this way is shown in Fig. 1. To obtain sufficient Auger-electron counts, the coincidence data sets were recorded at three different photon energies as indicated in Fig. 1. The pass energy of the analyzer was set to E_{pass}=100 eV for the S 2*p* ionization, while for the C and O 1*s* ionization they were set to E_{pass}=240 eV. The resolving power of the energy analyzer was estimated to be better than $E_{pass}/\Delta E$=100.

Figure 2 shows the coincidence and conventional Auger spectra plotted in a binding energy scale. In order to obtain the coincidence spectra, the electron-ion coincidences are filtered by the time window corresponding to the flight time of the metastable OCS^{2+} (~3.5 μs). In this analysis, false coincidence signals due to uncorrelated particles were carefully subtracted from the raw data. The red curves depict conventional spectra while the blue curves represent the coincidence Auger spectra related to the metastable dications. The intensities are normalized to the conventional spectra, and thus the spectral intensities directly reflect the decay branching ratios.

The coincidence observation has revealed metastable character of the Auger final doubly charged states lying in the range 30 - 35 eV which are attributed to the valence two-hole $3\pi^{-2}$ states [3]. The metastable yields show dramatic increase in the S 2*p* core-hole creation. This intense production is qualitatively explained by considering the spatial distribution of the 3π orbital involved in the decay processes. Since the 3π valence orbital is mostly localized around the S atom in the OCS molecule [4], the 3π electron preferentially fills the S 2*p* core-hole due to a large overlap between the core and valence orbitals. Thus the Auger transition involving the 3π electrons is favored in the decay of the S 2*p* core-hole states rather than in those of the C and O core-hole states.

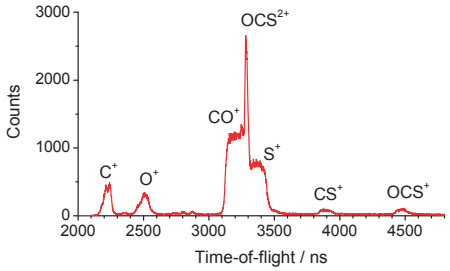

Fig. 1. TOF spectrum of ions measured in coincidence with sulfur LVV Auger electrons.

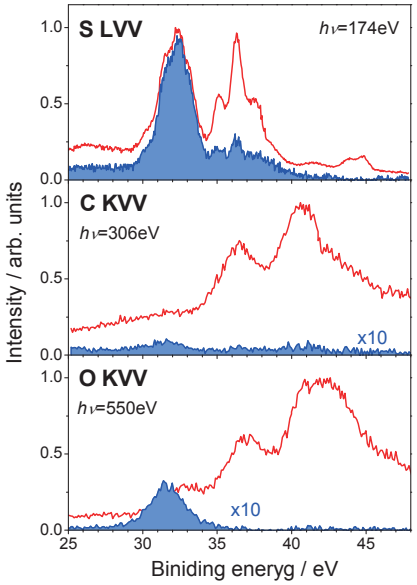

Fig. 2. Conventional (red curves) and coincidence (blue curves) Auger spectra of OCS. The coincidence spectra are extracted from the Auger-electron-ion coincidence data sets by filtering the Auger electron signals related to the formation of metastable OCS^{2+}.

[1] R. Feng *et al.*, Chem. Phys. **255** (2000) 353.
[2] T. Kaneyasu *et al.*, J. Electron Spectrosc. Relat. Phenom. **156-158** (2007) 279.
[3] T.X. Carroll *et al.*, J. Electron Spectrosc. Relat. Phenom. **51** (1990) 471.
[4] K.T. Leung, C.E. Brion, Chem. Phys. **96** (1985) 241.

BL4B

Stability and Dissociation of OCS^{2+} Formed via Auger Decays of S 2*p* Core-Hole States in OCS

T. Kaneyasu[1], M. Ito[1,2], Y. Hikosaka[1], E. Shigemasa[1]

[1]*UVSOR Facility, Institute for Molecular Science, Okazaki 444-8585 Japan*

[2]*Graduate School of Science and Technology, Niigata University, Niigata 950-21 Japan*

Auger decay is the main relaxation process following core ionization in molecules composed of light atoms. In the decay process, a valence electron fills the core-hole while another valence electron is ejected. Doubly charged molecules with two holes in the valence orbital, thus formed, often dissociate due to the Coulomb repulsion between the nuclear charges. The coincidence detection between the energy-selected Auger electrons and fragments ions is one of the most useful methods to gain a clear insight in the dissociation mechanism of the Auger final doubly charged states. We have developed an Auger-electron-ion coincidence spectrometer in which a toroidal electron energy analyzer and an ion momentum spectrometer are installed. In this report, we present a coincidence study on stability and dissociation of the Auger final states following the S 2*p* ionization of OCS.

The experiment was carried out on the beamline BL4B at the UVSOR facility. A detailed description of the spectrometer and data acquisition scheme were given in a previous paper [1]. An electron-ion coincidence data set was obtained for OCS at a photon energy of 174 eV corresponding to 2.15 eV above the S $2p_{1/2}$ threshold. Pass energy of the electron analyzer was set to E_{pass}=100 eV and the resolving power was evaluated to be better than $E_{pass}/\Delta E$ = 100. From the coincidence data set, we have extracted sulfur LVV Auger spectra for individual dissociation channels.

Figure 1(a) shows a conventional sulfur LVV Auger spectrum. Due to the spin-orbit splitting of the S 2*p* core-hole states (1.2 eV), the Auger spectrum is composed of two spectral components associated with individual core-hole states. The binding energy scale is calculated by subtracting the kinetic energy of Auger electrons from the ionization energy of the S $2p_{1/2}^{-1}$ core-hole state. Thus the scale is correct for the Auger lines related to the S $2p_{1/2}^{-1}$ state, but is shifted by 1.2 eV for those from the S $2p_{3/2}^{-1}$ state.

The spectrum shows band structures which are attributed to valence two-hole doubly charged states [2,3]. The assignment of the structures are denoted on the top of the spectrum. Auger electron spectra filtered by coincidences with OCS^{2+}, O^++CS^+ and $O+C^+$+S^+ are shown in Fig. 1(b)-1(d). The vertical bars in Figs. 1(c) and 1(d) indicate thermochemical thresholds for the ground states of the products. The intensities of the coincidence Auger spectra are normalized to that of the conventional spectrum, and thus the spectral intensity directly reflects the decay branching rations of the Auger final two-hole states. It is found that the $3\pi^{-2}$ states are mostly metastable, whose lifetimes should be much longer than the time-of-flight of OCS^{2+} (~3.5 μs) in the present spectrometer. The majority of the Auger final states around 36 eV corresponding to the $9\sigma^{-1}3\pi^{-1}$, $8\sigma^{-1}3\pi^{-1}$ and $2\pi^{-1}3\pi^{-1}$ states dissociates into CO^++S^+. The onset of this band structure exactly accords with the appearance potential (~34 eV) for the CO^++S^+ formation in valence double photoionization [4]. In the binding energy region above 40 eV, metastable OCS^{2+} can hardly be seen. The $9\sigma^{-1}2\pi^{-1}$ states in 40 - 43 eV predominantly dissociate into CO^++S^+. The high-lying states break apart into both the CO^++S^+ and $O+C^+$+S^+ fragments. The three-body dissociation arises only from the high-lying states.

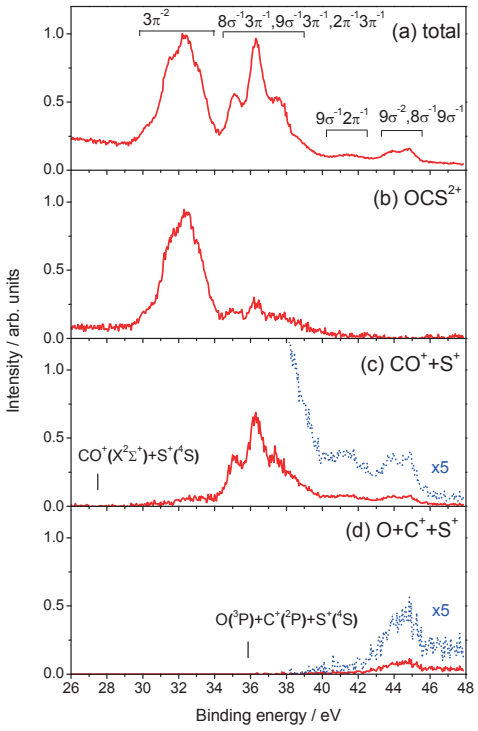

Fig. 1. (a) Conventional sulfur LVV Auger spectrum. Coincidence Auger spectra related to the formation of (b) metastable OCS^{2+}, (c) CO^++S^+ and (d) $O+C^+$+S^+.

[1] T. Kaneyasu *et al.*, J. Electron Spectrosc. Relat. Phenom. **156-158** (2007) 279.

[2] T. X. Carroll *et al.*, J. Electron Spectrosc. Relat. Phenom. **51** (1990) 471.

[3] D. Minneli *et al.*, J. Chem. Phys. **107** (1990) 6070.

[4] T. Masuoka, H. Doi, Phys. Rev. A **47** (1993) 278.